Macular Curvature in Adults Born Preterm With and Without ROP: Results from the Gutenberg Prematurity Eye Study

Achim Fieß,[1] Christin Volmering,[1] Sandra Gißler,[1] Eva Mildenberger,[2] Michael S. Urschitz,[3] Panagiotis Laspas,[1] Bernhard Stoffelns,[1] Norbert Pfeiffer,[1] and Alexander K. Schuster[1]

[1]Department of Ophthalmology, University Medical Center of the Johannes Gutenberg University Mainz, Mainz, Germany
[2]Division of Neonatology, Department of Pediatrics, University Medical Center of the Johannes Gutenberg University Mainz, Mainz, Germany
[3]Division of Pediatric Epidemiology, Institute for Medical Biostatistics, Epidemiology and Informatics, University Medical Center of the Johannes Gutenberg University Mainz, Mainz, Germany

Correspondence: Achim Fieß, Department of Ophthalmology, Medical Center of the Johannes Gutenberg University Mainz, Langenbeckstr. 1, Mainz 55131, Germany; achim.fiess@gmail.com.

Received: October 5, 2023
Accepted: February 19, 2024
Published: March 29, 2024

Citation: Fieß A, Volmering C, Gißler S, et al. Macular curvature in adults born preterm with and without ROP: Results from the gutenberg prematurity eye study. *Invest Ophthalmol Vis Sci.* 2024;65(3):39. https://doi.org/10.1167/iovs.65.3.39

Purpose. This study investigated the effects of prematurity and retinopathy of prematurity (ROP) as well as the associations of the ocular geometry with macular curvature in adults.

Methods. The Gutenberg Prematurity Eye Study is a retrospective cohort study of preterm and full-term participants aged 18 to 52 years with a prospective ophthalmologic examination. The main outcome measure was the macular curvature in the central foveal optical coherence tomography (OCT) scan and its associations with gestational age (GA), birth weight and birth weight percentile, ROP occurrence, ROP treatment, and other perinatal factors were evaluated in univariable and multivariable linear regression analyses. Furthermore, a second model assessed the association of ocular geometry with macular curvature.

Results. In the present study, 550 eyes of 284 adults born preterm and 277 eyes of 139 adults born full-term were examined (aged = 28.7 ± 8.7 years, 240 female subjects). In multivariable analyses for perinatal parameters, ROP treatment (B = −52.44, $P = 0.023$) and maternal smoking during pregnancy (B = 26.41, $P = 0.019$) showed an association with macular curvature. Regarding ocular geometric parameters, posterior segment length (B = 9.07, $P < 0.001$) and subfoveal choroidal thickness (B = −0.26, $P < 0.001$) were associated with macular curvature, central corneal thickness, anterior chamber depth, lens thickness, and foveal retinal thickness were not associated.

Conclusions. Adults treated for ROP had relatively more negative curvature values compared to the full-term group, indicating a macular protrusion toward the vitreous cave. A thicker subfoveal choroidal thickness was associated with a flatter macular curvature, whereas a longer posterior segment length was associated with a steeper macular curvature indicating the characteristics of the myopic elongation of the eye.

Keywords: birth weight, gestational age (GA), retinopathy of prematurity (ROP), dome-shaped macula, macular curvature, epidemiology

Preterm birth is increasing and globally affects about 11% of all newborns.[1] The ophthalmic outcomes of individuals born preterm range from no or mild comorbidities, such as a higher frequency of refractive error,[2–5] to severe comorbidities, such as the development of retinopathy of prematurity (ROP), which is a major cause of preventable blindness in childhood.[6] Many morphological eye alterations have been reported in those born prematurely or of low birth weight and are not only present in infancy and childhood but extend into adulthood. Besides differences in the anterior pole of the eye, such as altered steeper corneal shape and thicker lens anatomy,[7–9] there have been many findings concerning the posterior pole, ranging from alterations of the optic disc, such as a larger vertical cup-to-disc ratio[10] and thinner peripapillary retinal nerve fiber layer[11] to a thicker foveal shape,[12] an increased proportion of foveal hypoplasia,[12] and an altered configuration of the foveal avascular zone.[13–15]

A recent investigation by Legocki and colleagues of 37 infants after birth and with a 9-month follow-up suggests a connection among low birth weight, severe ROP, and macular curvature, specifically a dome-shaped macula.[16] A dome-shaped macula is a convex macular protrusion at the posterior pole instead of the normal concave course.[17] It has been primarily, but not exclusively, described in connection to posterior staphyloma and severe myopia[17,18] the latter being one of the multiple sequelae of premature birth.[2–5] However, these findings were in infants who had been screened for ROP, and, to our knowledge, there have been no studies analyzing the macular curvature in connection to premature

birth and low birth weight in adults. For this reason, the present study was designed to examine the macular curvature of adults born preterm to investigate whether the findings of Legocki and colleagues in infants could also be traced in later life. The correlations of macular curvature with different segments of ocular geometry were assessed as they may potentially play a role in the development of further maculopathy or retinal detachment, which occurs more often in highly myopic patients[19] but also in patients treated for ROP in later life.[20,21]

Materials and Methods

Study Population

The Gutenberg Prematurity Eye Study (GPES) is based at the University Medical Center of the Johannes Gutenberg University Mainz (UMCM) in Germany and examined a single-center-cohort of 18 to 52-year-old adults born preterm or at term (between 1969 and 2002) for the effects of prematurity on the eyes in adults. It is a retrospective cohort study with a prospective ophthalmologic examination. Potential participants were selected by an algorithm inviting every former preterm newborn with a gestational age at birth (GA) ≤32 weeks and every second randomly chosen preterm newborn with a GA of 33 to 36 weeks. Additionally, study controls of 6 randomly selected full-term subjects (3 male subjects and 3 female subjects for each month of the calendar) with a birth weight between the 10th and 90th percentile were also recruited as previously reported.[2,22–27] The flow chart for eligibility and the effective recruitment efficacy proportion is displayed in Supplementary Figure S1. The participants were examined between 2019 and 2021 and surveyed to gain insight into their medical history. In addition, their perinatal and postnatal histories stored in the UMCM were reviewed.

Written informed consent was obtained from all participants before their study entry. The GPES complies with Good Clinical Practice (GCP), Good Epidemiological Practice (GEP), and the ethical principles of the Declaration of Helsinki. The study protocol and study documents were approved by the local ethics committee of the Medical Chamber of Rhineland-Palatinate, Germany (reference no. 2019-14161; original vote: May 29, 2019, latest update: April 2, 2020).

Assessment of Pre-, Peri-, and Postnatal Medical History

All relevant information contained in the medical records stored at the UMCM was reviewed and the following data were collected: GA (weeks), birth weight (kg), presence of ROP, stage of ROP, ROP treatment, placental insufficiency, pre-eclampsia, breastfeeding, maternal smoking during pregnancy, and perinatal adverse events. For the present study, birth weight percentiles were calculated according to Voigt et al.[28]

Categorization

To gain insight into different stages of prematurity as well as ROP as its sequela, descriptive analysis was conducted stratified for 6 groups: participants born full-term with a GA at birth ≥37 completed weeks (group 1), preterm participants with GA of 33 to 36 weeks without ROP (group 2), GA of 29 to 32 weeks without ROP (group 3), GA ≤28 weeks without ROP (group 4), GA ≤32 and non-treated ROP (group 5), and treated ROP (group 6). In the case that only one eye was affected with ROP, the other non-ROP eye was excluded from the analysis.

Ophthalmologic Examination

The detailed ophthalmologic examination included testing of distant corrected visual acuity (DCVA) with ARK-1s (NIDEK; Oculus, Wetzlar, Germany) and the measurement of central corneal thickness, corneal radius, anterior chamber depths, posterior segment length, and axial length with LenStar (Lenstar LS900; Haag-Streit, Bern, Switzerland). Additionally, the intraocular pressure was measured with a non-contact tonometer (NT 2000; Nidek Co., Japan). According to medical literature, the visual acuity was converted from decimal to logMAR.[29]

Optical Coherence Tomography

For macular optical coherence tomography (OCT) imaging, the spectral-domain OCT (SD-OCT; OCT2; Heidelberg Engineering, Heidelberg, Germany) was used for a block scan 15 × 15 degrees in the enhanced depth imaging (EDI)-modus and 7.7 mm corneal curvature. The automatic segmentation was performed by a research software tool of the Heidelberg Eye Explorer Software (HEYEX; SPX, Heidelberg Engineering, Heidelberg, Germany) which segmented the retinal thickness of the macula as well as each retinal layer separately. This included measurements in microns in the fovea of the total retinal (TR) layer. The foveal center was defined as the deepest foveal depression and the foveal retinal thickness was defined as the minimum foveal retinal thickness in the foveal center. All SD-OCT measurements were performed in a darkened room on non-mydriatic eyes. Each scan was checked by a board-certified ophthalmologist for decentration or layer segmentation errors, and eyes with such errors were excluded. Thus, the present study only includes high-quality images with ideal centration, a high signal strength of >15 dB, and accurate automated delineation. In addition, foveal scans of both eyes were evaluated by two independent graders (authors A.K.S. and S.G.) for the presence of foveal hypoplasia, which was defined according to a previous report.[30] In the case of deviating gradings, the grading was determined by a third board-certified grader (author A.F.). Foveal hypoplasia was judged and categorized into 4 types: grade 1 was defined as a shallow foveal pit, the presence of a wider outer nuclear layer (ONL), and outer segment lengthening; grade 2 showed the characteristics of grade 1 but with the absence of a foveal pit; grade 3 was defined as grade 2 but with the absence of outer segment lengthening; and grade 4 was defined as the characteristics of grade 3 but with the absence of ONL widening.[30]

Definition of the Macular Curvature

For macular curvature calculations, we used 1:1 µm-ratio central foveal OCT scans which were exported after validation of proper automatic segmentation of the Bruch's membrane (BM; by HEYEX-Software, Heidelberg Engineering, Heidelberg, Germany) as well as upright and central centration. In the cases of good scan quality but not adequate BM segmentation, the BM segmentation was adjusted manually. The macular curvature was calculated

based on the BM segmentation line. To avoid errors in the border area, any remaining "BM" tags were deleted by automatically cutting 60 pixels from each side of the OCT scan. A quadratic polynomial fit (x^2) was performed and the second derivative thereof was used for curvature analysis. A quadratic function was used as the OCT scans did not include wide-field imaging, thus inflection points for dome height measurements were not within the scan range. We therefore decided to only calculate curvature values and negative curvature values would implicate a protrusion toward the vitreous cave (as would be expected in dome-shaped maculopathy [DSM]). In addition to curvature analysis, R^2 values of the polynomial fit were evaluated for quality assurance of the fitting procedure.

Inclusion and Exclusion Criteria

In the present analysis, only participants with a sufficient quality of the central foveal SD-OCT scan and a sufficient polynomial fit (mean $R^2 = 0.99$ of all OCT scans, minimal $R^2 = 0.74$) of BM lines were included in the analysis.

Covariables

Two different aspects of macular curvature were evaluated: first, factors that may affect the macular curvature with a specific focus on perinatal parameters including GA (weeks), birth weight (kg), birth weight percentile, ROP, ROP treatment, placental insufficiency, pre-eclampsia, maternal smoking, breastfeeding, and perinatal adverse events. Perinatal adverse events were defined according to the German query for quality control of the neonatal clinics: occurrence of intraventricular hemorrhage (at least grade 3 or parenchymal hemorrhage), the occurrence of necrotizing enterocolitis, and moderate or severe bronchopulmonary dysplasia were summarized as adverse events. In the second step, we analyzed the relationship of macular curvature with geometric features of the eye, such as central corneal thickness (µm), anterior chamber depth (µm), lens thickness (µm), posterior segment length (µm), foveal retinal thickness, and subfoveal choroidal thickness.

Statistical Analysis

The main outcome measure was the macular curvature defined by the second derivative of a quadratic polynomial fit of the automatically generated BM segmentation. The polynomial fit was calculated using R (R Core Team [2021]; R: A language and environment for statistical computing. R Foundation for Statistical Computing, Vienna, Austria, URL https://www.R-project.org/, R version 4.1.2 [2021-11-01]). Descriptive statistics were computed and stratified by the clinical group. Absolute and relative frequencies were calculated for dichotomous parameters, and the mean and standard deviation were calculated for approximately normally distributed variables (otherwise median and interquartile range). Linear regression models with general estimating equations (GEEs) were used to assess associations and account for correlations between corresponding eyes. As previous authors have mentioned in their research with a Topcon OCT, raster scans did not undergo any sort of spatial processing, however, we do not know if this also accounts for imaging post-production in the HEYEX algorithm as well. Furthermore, as also pointed out by Müller et al., varying optical path distortions by OCT system optics could not be excluded.[31] We have therefore decided to also adjust for mean corneal power as well as axial length to account for these possible influences in the perinatal model. For the ocular morphology model, we broke down the highly associated axial length into central corneal thickness, lens thickness, anterior chamber depth, and posterior segment length. First, univariable analyses of the macular curvature and sex (female), age (years), mean corneal power (diopter), axial length (mm), GA (weeks), birth weight (kg), birth weight percentile, ROP (yes), ROP treatment (yes), perinatal adverse events (yes), placental insufficiency (yes), pre-eclampsia (yes), breastfeeding, (yes) and maternal smoking during pregnancy (yes) were computed. Additionally, we calculated univariable models with adjustment for age, sex, axial length, and mean corneal power. Then, only perinatal parameters associated in the univariable analyses were included in the first multivariable model with additional adjustments for sex, age, corneal power, and axial length, but excluding ROP treatment due to high collinearity of ROP and ROP treatment. In the second multivariable model, multivariable associated perinatal parameters and the potential effect of ROP treatment (yes) were analyzed with additional adjustments for age, sex, axial length, and mean corneal power. Birth weight was excluded from the multivariable models to avoid collinearity, which was strong between GA at birth and birth weight. In the analysis of ocular geometry, the associations of ocular geometry with macular curvature were analyzed including only subjects without ROP treatment. First, univariable associations were calculated between macular curvature and sex (female), age (years), mean corneal power (diopter), central corneal thickness (µm), anterior chamber depth (mm), lens thickness (mm), posterior segment length (mm), foveal retinal thickness (µm), and subfoveal choroidal thickness (µm). We then calculated univariable models with additional adjustments for age, sex, and mean corneal power. In the multivariable model, all ocular geometric parameters were included that were associated in univariable analyses with additional adjustments for age, sex, and mean corneal power. A sensitivity analysis was performed with the inclusion of foveal hypoplasia in the model testing the association with ocular geometry. As this is an explorative study, a significance level was not defined and no adjustment for multiple testing was conducted. Thus, *P* values are reported only for descriptive purposes and should be interpreted with caution.[32] Calculations were performed using commercial software (IBM SPSS 20.0; SPSS, Inc., Chicago, IL, USA).

Results

Participant Characteristics

In the present study, 550 eyes of 284 individuals born preterm and 277 eyes of 139 individuals born full-term were examined (aged = 28.7 ± 8.7 years, 240 female subjects) and the characteristics of the different groups are described in Table 1. In the group treated for ROP, six participants (11 eyes) underwent laser coagulation treatment and four participants (7 eyes) had cryocoagulation. Regarding perinatal factors, as expected, birthweight was lower in groups with individuals born preterm compared to individuals born full-term. The perinatal parameters are described in Table 1 and Table 2 presents the ocular geometric parameters. The

Table 1. Characteristics of the GPES Sample (n = 423) Stratified by Study Groups

Gestational Age	Group 1 GA ≥ 37	Group 2 GA 33–36 No ROP	Group 3 GA 29–32 No ROP	Group 4 GA ≤ 28 No ROP	Group 5 GA ≤ 32 ROP Without Treatment	Group 6 GA ≤ 32 ROP With Treatment
Participants (n)/eyes (n)	**139/277**	**135/268**	**87/170**	**15/28**	**37/66**	**10/18**
Gender (women)	81 (58.3%)	81 (60.0%)	46 (52.9%)	7 (46.7%)	21 (56.8%)	4 (40.0%)
Age, y	29.9 ± 9.1	29.4 ± 9.2	28.6 ± 8.0	23.7 ± 8.0	24.6 ± 5.6	27.4 ± 6.2
Birth weight, g	3422 ± 392	2072 ± 466	1552 ± 330	947 ± 191	1085 ± 393	862 ± 272
Birth weight < 1500 g (yes)	0 (0%)	13 (9.6%)	36 (41.4%)	15 (100%)	31 (83.8%)	10 (100%)
Birth weight < 1000 g (yes)	0 (0%)	0 (0%)	5 (5.7%)	8 (53.3%)	16 (43.2%)	7 (70%)
Birth weight percentile	48.6 ± 21.5	25.4 ± 24.3	44.4 ± 24.3	45.7 ± 22.3	38.8 ± 28.7	27.8 ± 26.1
Gestational age (wk)	39.3 ± 1.3	34.3 ± 0.96	30.6 ± 1.2	26.5 ± 1.6	28.8 ± 2.1	27.1 ± 2.7
(min-max)	(37–43)	(33–36)	(29–32)	(23–28)	(24–32)	(24–32)
ROP stage (1/2/3)	0/0/0	0/0/0	0/0/0	0/0/0	31/31/4	0/3/15
Perinatal adverse events (yes)*	1 (0.7%)	3 (2.2%)	5 (5.7%)	1 (6.7%)	11 (29.7%)	7 (70.0%)
Intraventricular hemorrhage (yes) #	0 (0%)	0 (0%)	0 (0%)	1 (6.7%)	0 (0%)	0 (0%)
Bronchopulmonary dysplasia (yes)+	1 (0.7%)	0 (0%)	4 (4.6%)	0 (0%)	8 (21.6%)	3 (30.0%)
Necrotizing entercolitis (yes)	0 (0%)	3 (2.2%)	1 (1.1%)	1 (6.7%)	3 (8.1%)	5 (50.0%)
Pre-eclampsia (yes)	10 (7.2%)	24 (17.8%)	10 (11.5%)	3 (20.0%)	7 (18.9%)	3 (30.0%)
Placental insufficiency (yes)	2 (1.4%)	16 (11.9%)	2 (2.3%)	0 (0%)	2 (5.4%)	0 (0%)
HELLP syndrome	0 (0%)	6 (4.4%)	1 (1.1%)	0 (0%)	2 (5.4%)	0 (0%)
Maternal smoking (yes)##	7 (5.0%)	8 (5.9%)	8 (9.2%)	1 (6.7%)	3 (8.1%)	2 (20%)
Gestational diabetes (yes)	1 (0.7%)	7 (5.2%)	1 (1.1%)	1 (6.7%)	1 (2.7%)	0 (0%)
Breastfeeding (yes)	77 (56.1%)	74 (54.8%)	43 (49.4%)	8 (53.3%)	18 (48.6%)	5 (50.0%)
Ocular parameters						
Visual acuity (LogMAR) OD	0.0 (0.0 to 0.0)	0.0 (0.0 to 0.0)	0.0 (0.0 to 0.0)	0.0 (0.0 to 0.0)	0.0 (0.0 to 0.0)	0.0 (0.0 to 0.1)
Visual acuity (LogMAR) OS	0.0 (0.0 to 0.0)	0.0 (0.0 to 0.0)	0.0 (0.0 to 0.0)	0.0 (0.0 to 0.0)	0.0 (0.0 to 0.1)	0.1 (0.0 to 0.3)
Spherical equivalent (diopter) OD	−0.94 ± 2.13	−1.14 ± 2.17	−0.69 ± 2.18	−0.71 ± 1.96	−0.86 ± 2.06	−2.11 ± 3.36
Spherical equivalent (diopter) OS	−0.97 ± 2.09	−1.22 ± 2.13	−0.95 ± 2.59	−0.58 ± 2.20	−1.03 ± 1.88	−0.57 ± 4.34
Intraocular pressure (mm Hg) OD	15.4 ± 2.8	14.6 ± 3.0	15.1 ± 3.3	16.0 ± 3.2	15.8 ± 3.5	16.9 ± 4.6
Intraocular pressure (mm Hg) OS	15.2 ± 2.8	14.5 ± 3.0	14.6 ± 2.9	15.0 ± 3.2	16.0 ± 3.6	15.6 ± 3.6

g, gram; GA, gestational age; mm, millimeter; n, number; OD, right eye; OS, left eye, ROP, retinopathy of prematurity; y, years, Visual acuity is described as median and interquartile range.

* Perinatal adverse events were defined as the occurrence of intraventricular hemorrhage# (at least grade 3 or parenchymal hemorrhage) and/or occurrence of necrotizing enterocolitis and/or bronchopulmonary dysplasia (+moderate or severe). ##: maternal smoking during pregnancy.

recruitment efficacy proportion for each group is presented in Supplementary Figure S1. Furthermore, eight eyes without ROP were excluded in which the fellow eye was affected with postnatal ROP. The participants' characteristics are described in Table 1.

Descriptive Curvature Measures

The treated ROP group had a significantly lower macular curvature than the control group (P < 0.001), whereas the other preterm groups were not significantly different from the full-term controls (see Fig. 1). Furthermore, the proportion of participants with negative curvature was descriptively higher in the ROP-treated group compared to the control group.

Association Analyses of Perinatal History

Macular curvature was associated with female gender (B = 18.64, 95% confidence interval [CI] = 9.95 to 27.3, P < 0.001), axial length (B = 10.29, 95% CI = 4.52 to 16.1, P < 0.001), ROP (B = −23.4, 95% CI = −41.3 to −5.52, P = 0.01), ROP treatment (B = −76.42, 95% CI = −112.3 to −40.5, P < 0.001), perinatal adverse events (B = −33.63, 95% CI = −47.7 to −19.6, P < 0.001) in univariable analysis using generalized linear regression models. In the multivariable model including all univariable associated parameters (with exception of ROP treatment), perinatal adverse events (B = −21.26, 95% CI = −37.57 to −4.95, P = 0.011), and smoking during pregnancy (B = 25.31, 95% CI = 3.45 to 47.2, P = 0.023), remained associated. In multivariable model 3, ROP treatment (B = −52.44, 95% CI = −97.64 to −7.25, P = 0.023) and maternal smoking during pregnancy (B = 26.41, 95% CI = 4.40 to 48.41, P = 0.019) were significantly associated with macular curvature after adjusting for age, sex, mean corneal power, and axial length (Table 3).

Association Analyses of Ocular Geometry

The following ocular geometric parameters revealed an association with macular curvature in univariable analyses: posterior segment length (B = 11.36, 95% CI = 5.36 to 17.4, P < 0.001), foveal retinal thickness (B = −0.21, 95% CI = −0.39 to −0.04, P = 0.02) and subfoveal choroidal thickness (B = −0.26, 95% CI = −0.35 to −0.18, P < 0.001). In multivariable analysis models after additional adjustment for sex, age, and mean corneal power, macular curvature was associated with posterior segment length (B = 9.07, 95% CI = 3.69 to 14.45, P < 0.001) and subfoveal choroidal thickness (B = −0.26, 95% CI = −0.33 to −0.19, P < 0.001; Table 4 and Fig. 2).

Table 2. Geometrical Parameters of the Eye and Curvature Parameters for the GPES Sample ($n = 423$) for Each Study Group

Gestational Age	Group 1 GA ≥ 37	Group 2 GA 33–36 No ROP	Group 3 GA 29–32 No ROP	Group 4 GA ≤ 28 No ROP	Group 5 GA ≤ 32 ROP Without Treatment	Group 6 GA ≤ 32 ROP With Treatment
Participants/eyes (*n*)	**139/277**	**135/268**	**87/170**	**15/28**	**37/66**	**10/18**
Curvature ($2*Coeffx^2*10^6$) OD	80.9 ± 65.8	84.7 ± 67.3	81.5 ± 67.7	78.9 ± 55.5	67.7 ± 62.7	9.4 ± 87.9
Curvature ($2*Coeffx^2*10^6$) OS	81.5 ± 55.8	82.9 ± 53.8	90.8 ± 78.0	67.9 ± 30.9	78.9 ± 88.6	10.8 ± 68.8
Negative curvature OD	12 (8.7%)	3 (2.2%)	7 (8.1%)	0 (0%)	4 (12.1%)	3 (30%)*
Negative curvature OS	6 (4.3%)	3 (2.3%)	5 (6.0%)	0 (0%)	3 (9.1%)	3 (37.5%)*
Ocular geometry						
Central corneal thickness (µm) OD	550.8 ± 36.6	539.3 ± 35.6	543.2 ± 41.3	544.3 ± 42.5	550.0 ± 43.3	563.9 ± 47.4
Central corneal thickness (µm) OS	551.6 ± 37.8	538.8 ± 32,8	541.0 ± 39.3	542.4 ± 42.5	551.6 ± 47.4	555.5 ± 49.6
Corneal radius (mm) OD	7.89 ± 0.30	7.80 ± 0.31	7.71 ± 0.31	7.74 ± 0.22	7.62 ± 0.32	7.65 ± 0.27
Corneal radius (mm) OS	7.88 ± 0.32	7.79 ± 0.30	7.72 ± 0.31	7.73 ± 0.23	7.62 ± 0.29	7.58 ± 0.29
Anterior chamber depth (mm) OD	2.93 ± 0.33	3.02 ± 0.32	3.03 ± 0.29	2.96 ± 0.21	3.01 ± 0.47	2.57 ± 0.67
Anterior chamber depth (mm) OS	2.94 ± 0.33	3.03 ± 0.33	3.03 ± 0.34	2.90 ± 0.29	3.00 ± 0.35	2.26 ± 0.44
Lens thickness (mm) OD	3.78 ± 0.34	3.78 ± 0.33	3.76 ± 0.26	3.71 ± 0.24	3.62 ± 0.22	4.39 ± 0.47
Lens thickness (mm) OS	3.76 ± 0.34	3.77 ± 0.32	3.75 ± 0.32	3.73 ± 0.26	3.61 ± 0.25	4.39 ± 0.51
Posterior segment length (mm) OD	17.0 ±1.12	16.9 ± 1.09	16.6 ±1.04	16.7 ± 0.69	16.6 ± 0.94	16.0 ± 1.98
Posterior segment length (mm) OS	17.0 ± 1.13	16.8 ± 1.01	16.7 ±1.02	16.4 ± 0.99	16.5 ± 0.78	14.6 ± 1.05
Axial length (mm) OD	23.7 ± 1.19	23.7 ± 1.15	23.4 ± 1.07	23.4 ± 0.74	23.2 ± 1.19	22.5 ± 1.80
Axial length (mm) OS	23.7 ± 1.18	23.6 ± 1.09	23.4 ± 1.04	23.0 ± 1.06	23.3 ± 1.18	21.9 ± 1.51
Geometry posterior segment						
Total retinal thickness (µm) OD	275.0 ± 20.1	282.9 ± 18.8	294.8 ± 24.6	310.4 ± 20.4	297.9 ± 20.5	328.1 ± 35.1
Total retinal thickness (µm) OS	274.8 ± 20.3	282.9 ± 19.0	296.4 ± 27.5	311.6 ± 21.7	301.5 ± 40.2	308.9 ± 23.7
Subfoveal choroidal thickness (µm) OD	282.9 ± 66.6	295.1 ± 65.0	284.6 ± 64.5	304.3 ± 62.0	316.1 ± 78.1	297.5 ± 88.0
Subfoveal choroidal thickness (µm) OS	288.0 ± 73.2	288.0 ± 60.9	290.6 ± 68.8	340.3 ± 64.5	298.3 ± 75.1	297.0 ± 56.7
Foveal hypoplasia (yes) OD	3 (2.2%)	13 (9.6%)	15 (17.4%)	7 (50.0%)	17 (51.5%)	7 (70.0%)
Foveal hypoplasia (yes) OS	2 (1.4%)	11 (8.3%)	16 (19.0%)	7 (50.0%)	14 (42.2%)	5 (62.5%)

GA, gestational age; *n*, number; OD, right eye; OS, left eye; ROP, retinopathy of prematurity; * - significant difference between ROP-treated group (group 6) and group 1 (p (OD) = 0.03; p(OS) < 0.001).

For increasing the understanding of the resulting small curvature values, we chose to use a different dimension and therefore multiplied the values by 10^6 before analyzing.

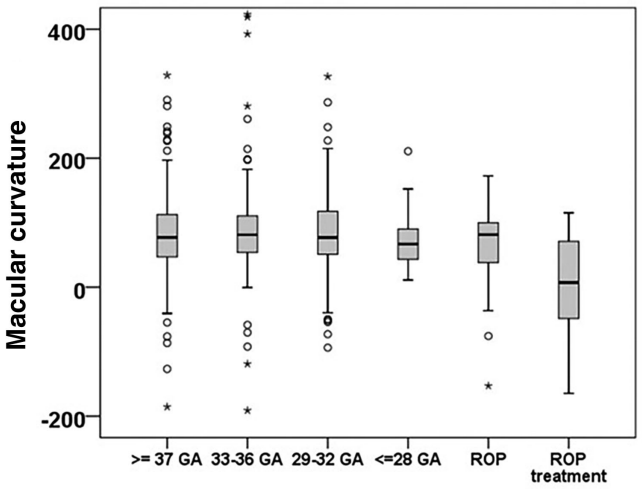

Figure 1. Retinal curvature distribution ($n = 423$) stratified by study groups. Individuals with treated ROP had lower retinal curvature values. Legend: GA – gestational age; ROP – retinopathy of prematurity. For increasing the understanding of the resulting small curvature values, we chose to use a different dimension and therefore multiplied the values by 10^6 before analyzing.

Sensitivity Analysis

A sensitivity analysis was conducted the presence of hypoplasia in the uni- and multivariable models for ocular geometry. However, there was no association observed between foveal hypoplasia and macular curvature. Furthermore, when geometric parameters such as posterior segment length and subfoveal choroidal thickness were included in the multivariable model of perinatal parameters, the association between macular curvature and ROP treatment was not significant ($P = 0.2$).

Discussion

Our analyses demonstrate that ROP therapy as well as maternal smoking during pregnancy were associated with macular curvature in young to middle-aged adults, indicating that not prematurity itself but its sequelae and concomitant diseases and treatment affect macular development regarding the curvature. Furthermore, subfoveal choroidal thickness was negatively correlated, whereas the posterior segment length was positively correlated with macular curvature, which could be connected to the myopic elongation of the eye.

Only one study has assessed the association between low birth weight, severe ROP, and macular curvature, specifically a dome-shaped macula[16] in 37 preterm infants (mean GA = 27.8 ± 3.2, birthweight = 949 ± 284 g) who were screened for ROP. Like Legocki et al.,[16] we did not find an association between GA and macular curvature. These authors, in contrast to our data, found a relationship with low birth weight but their data were limited because they only examined children born very preterm and no full-term

Table 3. Association Analyses of the Curvature Distribution (Complete Case Analysis: Eyes = 823) and Perinatal History in the GPES Sample (GEE)

	Univariable		model 1		model 2		model 3	
	B [95% CI]	***P* Value**	**B [95% CI]**	***P* Value**	**B [95% CI]**	***P* Value**	**B [95% CI]**	***P* Value**
Curvature coefficient* 10^6								
Age, y	−0.38 [−0.99 to 0.23]	0.22	−0.54 [−1.12 to 0.03]	0.063	−0.62 [−1.22 to 0.02]	0.044	−0.56 [−1.13 to 0.01]	0.056
Sex (female)	18.64 [9.95 to 27.3]	<0.001	22.12 [13.12 to 31.12]	<0.001	20.84 [11.90 to 29.77]	<0.001	20.02 [11.18 to 28.86]	<0.001
Mean corneal power	0.03 [−0.25 to 0.31]	0.82	0.09 [−0.17 to 0.35]	0.49	0.05 [−0.21 to 0.33]	0.68	0.09 [−0.18 to 0.35]	0.53
Axial length	10.29 [4.52 to 16.1]	<0.001	11.88 [6.20 to 17.56]	<0.001	10.91 [5.00 to 16.82]	<0.001	10.48 [4.6 to 16.36]	<0.001
Gestational age (weeks)	0.96 [0.002 to 1.92]	0.05	0.45 [−0.66 to 1.57]	0.427				
Birth weight (kg)	2.67 [−1.72 to 7.07]	0.23	0.94 [−4.03 to 5.9]	0.712	*	*	*	*
Birth weight percentile	−0.01 [−0.16 to 0.15]	0.94	−0.04 [−0.19 to 0.11]	0.594				
ROP (yes)	−23.41 [−41.3 to −5.52]	0.01	−18.83 [−38.22 to 0.56]	0.06	−12.79 [−34.46 to 8.88]	0.25		
ROP treatment (yes)	−76.42 [−112.3 to −40.5]	<0.001	−58.78 [−99.01 to −18.54]	0.004			−52.44 [−97.64 to −7.25]	0.023
Perinatal adverse events (yes)	−33.63 [−47.7 to −19.6]	<0.001	−24.88 [−39.28 to −10.49]	<0.001	−21.26 [−37.57 to −4.95]	0.011	−15.5 [−31.99 to 0.99]	0.07
Smoking during pregnancy (yes)	21.39 [1.6 to 44.4]	0.068	22.04 [0.23 to 43.86]	0.048	25.31 [3.45 to 47.2]	0.023	26.41 [4.40 to 48.41]	0.019
Pre-eclampsia (yes)	−5.13 [−15.3 to 5.08]	0.33	0.02 [−9.65 to 9.7]	0.996				
Breastfeeding (yes)	2.93 [−6.1 to 12.0]	0.52	0.98 [−8.01 to 9.96]	0.831				
Placental insufficiency (yes)	−3.91 [−20.7 to 12.9]	0.65	−7.46 [−23.88 to 8.97]	0.374				

B, beta estimates; CI, confidence interval.

Univariable model

Model 1: Univariable, adjusted for age, sex, axial length, and mean corneal power.

Model 2: Multivariable model with the inclusion of univariable associated parameters with adjustment for age, sex, axial length, and mean corneal power but not ROP treatment because of the strong correlation between ROP and ROP treatment.

Model 3: Multivariable model with the inclusion of associated parameters of model 2 and additional inclusion of ROP treatment.

* Because of high collinearity with gestational age, the parameter birth weight was not included in the multivariable models.

For increasing the understanding of the resulting small curvature values, we chose to use a different dimension and therefore multiplied the values by 10^6 before analyzing.

Table 4. Association Analyses of the Curvature Distribution and Geometrical Features in the GPES Sample (Excluding the ROP-Treated Participants, GEE)

	Univariable		Model 1		Model 2	
	B [95% CI]	***P* Value**	**B [95% CI]**	***P* Value**	**B [95% CI]**	***P* Value**
Curvature coefficient* 10^6						
Age	−0.6 [−1.16 to −0.04]	0.04	−0.6 [−1.17 to −0.34]	0.04	−0.92 [−1.44 to −0.4]	<0.001
Sex	14.6 [6.0 to 23.2]	0.001	14.71 [6.08 to 23.34]	<0.001	15.47 [6.77 to 24.18]	<0.001
Mean corneal power	0.14 [−0.13 to 0.41]	0.3	0.2 [−0.07 to −0.48]	0.14	0.09 [−0.16 to 0.35]	0.47
Central corneal thickness	−0.06 [−0.24 to 0.13]	0.53	−0.03 [−0.21 to 0.16]	0.76		
Anterior chamber depth	−7.32 [−22.3 to 7.63]	0.34	−9.68 [−24.23 to 4.87]	0.19		
Lens thickness	−1.98 [−19.1 to 15.1]	0.82	16.31 [−2.92 to 35.54]	0.1		
Posterior segment length	11.36 [5.36 to 17.4]	<0.001	12.01 [5.99 to 18.02]	<0.001	9.07 [3.69 to 14.45]	<0.001
Foveal retinal thickness	−0.21 [−0.39 to −0.04]	0.02	−0.13 [−0.31 to 0.05]	0.15	0.09 [−0.26 to 0.08]	0.3
Subfoveal choroidal thickness	−0.26 [−0.35 to −0.18]	<0.001	−0.29 [−0.37 to −0.21]	<0.001	−0.26 [−0.33 to −0.19]	<0.001
Axial length	9.34 [3.64 to 15.0]	0.001	10.79 [5.08 to 16.49]	<0.001	*	*

B, estimate in linear regression; CI, confidence interval.
Univariable model.
Model 1: Univariable, adjusted for age, sex, and mean corneal power.
Model 2: Multivariable model with the inclusion of univariable associated parameters with adjustment for age, sex and mean corneal power.
* We did not adjust for axial length in this model due to high collinearity of axial length and posterior segment length.

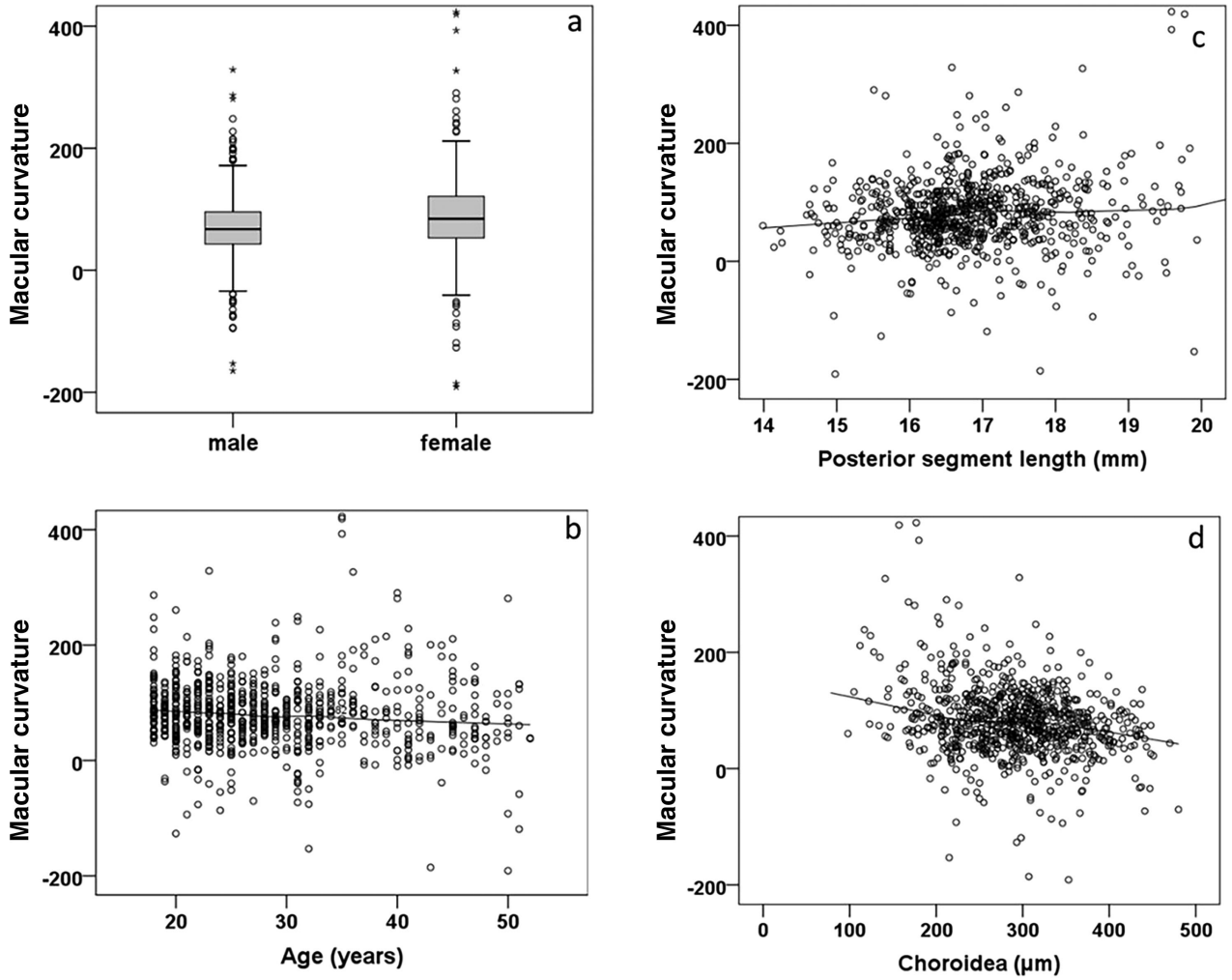

Figure 2. The relationship of retinal curvature distribution with (**a**) sex, (**b**) age, (**c**) posterior segment length, and (**d**) choroidal thickness. Participants with postnatal ROP treatment were excluded in panels **a** to **d**. For increasing the understanding of the resulting small curvature values, we chose to use a different dimension and therefore multiplied the values by 10^6 before analyzing.

Investigative Ophthalmology & Visual Science

controls and they did not differentiate between ROP-treated and non-treated individuals. The authors reported that their cases of plus-disease were also considered to be associated with macular curvature, which might be in congruence with our data in which we found an association with ROP treatment being necessary for individuals with severe ROP. Our data extend that of Legocki et al.[16] because we demonstrate that advanced ROP stages requiring treatment leads to lifelong changes in macular curvature. Furthermore, the present study provides new data showing that the different levels of prematurity do not affect macular curvature. Legocki et al. speculate that dome-shaped macula in general might be part of a natural developmental process that changes during further stages of development, consolidating their findings with Dubis et al. who described differences in OCT-based retinal curvature in children with postmenstrual age of 32 weeks to 4 years (39 children were included). In subjects aged 30 to 40 weeks postmenstrual, they found what they termed a "temporal divot" indicating an irregular growth of the sclera and retina during development.[33] The findings of Dubis et al. suggest an approach to "normal" configuration close to the time of the expected term birth, as they only found curvature differences up to 40 weeks postmenstrual age,[33] whereas our data provide evidence for lifelong alterations until adulthood in ROP treated individuals.

It is possible that ROP treatment with laser or cryotherapy alters the regular developmental process and might be a result of scarring tissue developed after treatment. Because the ROP treated group consisted mainly of participants with more advanced ROP, the association with treatment could also be influenced by the later ROP stage. In general, these findings are of interest as patients with ROP tend to have retinal tears even in adulthood,[21] which might also be partially explained by shear stress due to the changing shape of the globe.

Besides the theory of a change in macular curvature during the natural developmental processes in infancy, there are two other possible causes of a macular protrusion in later life, one of them being central additional tissue growth within the macular area, and the second being a further growth or loss of eye material in the perimacular area but reduced or missing in the central macula.[34,35] There have been many speculations about the development of a dome-shaped figure reaching from vitreomacular traction to differences in intraocular pressure,[36] as well as scleral or choroidal thickening/thinning,[34] which might also have contributed to the alterations in macular curvature in our ROP-treated individuals. Due to the limited depth resolution of SD-OCT scans in our study, unfortunately, it was not possible to evaluate the thickness of scleral tissue, however, we measured the subfoveal choroidal thickness, which was negatively associated with macular curvature, indicating that a larger subfoveal choroidal thickness could lead to a lesser macular curvature or even a macular protrusion. Furthermore, our results show a positive association of macular curvature with posterior segment length. This association connects to the theory of myopia development as axial eye elongation rather than symmetrical growth of the eye being involved in the development and progression of myopia.[37]

The significant association of maternal smoking during pregnancy might be explained by the previous findings of this study group, namely that maternal smoking during pregnancy was associated with subfoveal choroidal thinning.[38] Thus, the negative association of maternal smoking and subfoveal choroidal thickness also explains the association of maternal smoking with larger curvature values.

Our findings are supported by several studies investigating dome-shaped macula and myopia. Park and colleagues showed that there was a decrease in overall choroidal and scleral tissues when axial length increases in highly myopic eyes, when macular curvature became steeper or posterior staphyloma was diagnosed.[39] This was also reported by Ellabban and colleagues in their longitudinal study elaborating on the scleral and choroidal configuration in DSM.[34] Interestingly, Minami et al. found similar results in normal eyes reporting an association of macular curvature with choroidal thickness and axial length.[40] Caillaux et al. observed that the macular bulge height was positively correlated with the central choroidal thickness in their study examining 33 patients with DSM and decreased vision. They also found that choroidal thickness was significantly thicker in the foveal area than on the borders of the dome.[41] There might be a difference in the genesis or general kind of DSM depending on the vertical or horizontal configuration. As we only imaged our study participants with horizontal OCT scans, we cannot comment on the bulge shape of DSM. Some authors reported that the central choroidal thickness is the same in DSM and non-DSM groups and that the temporal and nasal choroidal thickness but not the subfoveal choroidal thickness were smaller in DSM individuals.[35] They proposed that macular protrusion seems to be due to macular fixation, whereas peripheral regions continue with growth in axial length.

All of the above-mentioned studies analyzed alterations in macular shape in relation to the choroidal thickness or axial length in study participants irrespective of birth history. However, Huang and colleagues analyzed infants born at term and did not find a correlation between subfoveal choroidal thickness and a dome-shaped macula. Although the subgroup with a dome-shaped macula in their small cohort of 39 infants included only 5 infants and their definition of the dome-shaped macula was different from previous studies, their findings indicate that changes in macular curvature due to choroidal thickness and axial length occur after birth and are not necessarily already relevant in infancy.[42] Thus, there might be different mechanisms involved in the development of macular curvature and a DSM shape in infancy that are not necessarily connected to changes in choroidal structure or axial length. Interestingly, Xiang et al. examined 19 Chinese children aged 4 to 6 years with DSM and found that the foveal avascular zone and perimeter were significantly positively correlated with the dome height.[43] This might not only be of interest in relation to the genesis of DSM but also play a role in the non-significance of our findings regarding macular curvature and GA, as it has been described in previous studies that children born preterm tend to have a smaller foveal avascular zone compared to children born at term.[14]

Strengths and Limitations

This study has several limitations. First, it was a single center-based design including primarily Caucasian participants and, hence, cannot be generalized to other populations. Additionally, we were not able to contact all former newborns. Furthermore, the sample size in our groups for ROP and ROP treatment are rather small and the treatment strategies have changed over time, with older partic-

ipants undergoing cryotherapy, whereas younger participants were treated with laser therapy. This limits the judgment of significance of our results. OCT imaging did not include wide-field scans, hence, our analysis is limited to the immediate perifoveal macular curvature shown in only one horizontal central foveal scan, thus, it was not possible to grade dome-shaped macula as this characteristic requires a three-dimensional approach. Consequently, we were not able to investigate other parameters such as dome height or measure possible associations between curvature configuration and characteristics of the sclera as SD-OCT imaging does not have a sufficient depth resolution. Although we have tried to correct for potentially influential factors on OCT image distortion, we cannot fully rule out distortions caused by the nature of the OCT measurement as described by Minami et al.[40,44] However, they used swept-source OCT (SS-OCT) which might produce a different distortion than our SD-OCT, especially as it enables more wide-field scans.

Nonetheless, this study also has several strengths. First, the study involved a large cohort of individuals born preterm, including young adults up to middle-aged participants of different stages of prematurity, birth weight, and ROP morbidity, and/or ROP treatment. The extensive review of medical charts as well as the inclusion of a detailed questionnaire provided a broad insight into the perinatal circumstances. Although other studies[40] took a manual approach to extracting coordinates for polynomial fit, we automatically extracted the segmented BM line. The advantages of using the BM line for curvature measurements compared to the RPE line are explained in detail by Miyake and colleagues.[45] Furthermore, measurements were conducted by investigators masked to the participants' birth history, thus, investigator-dependent bias was unlikely.

Conclusions

In conclusion, there is an association between a flatter macular curvature in individuals previously treated for ROP as well as an association of macular curvature with maternal smoking during pregnancy, while macular curvature was independent of GA, birthweight, or other perinatal factors regarding preterm birth. This association could be partially explained by ocular geometry including longer posterior segment length and differences in choroidal thickness, both factors associated with macular curvature indicating alterations due to myopic elongation of the eye.

Acknowledgments

The whole study team thanks all participants who took part in this study, and the whole GPES, which includes an enthusiastic team to explore perinatal factors on long-term eye development.

Fieß is supported by the Intramural Research Funding (Stufe I) of the University Medical Center of Johannes Gutenberg University Mainz. The present study was supported by the Ernst- und Berta-Grimmke Stiftung and the Else Kröner-Fresenius-Stiftung. The funders had no role in the study design, data collection and analysis, decision to publish, or preparation of the manuscript. Schuster AK holds the professorship for ophthalmic healthcare research endowed by "Stiftung Auge" and financed by "Deutsche Ophthalmologische Gesellschaft" and "Berufsverband der Augenaerzte Deutschlands e.V."

Authors' Contributions: Conceived and designed the study: A.F. and A.K.S. Analyzed the data: A.F., C.V., S.G., E.M., and A.K.S. Wrote the paper: A.F. Critically revised the manuscript: A.F., C.V., S.G., E.M., M.S.U., P.L., B.S., N.P., and A.K.S. All authors read and approved the final manuscript. This study contains parts of the thesis of Christin Volmering.

Access to Data, Responsibility, and Analysis: A.F. had full access to all study data and takes responsibility for the integrity of the data and the accuracy of the data analysis. Statistical analyses were performed by A.F. and S.G.

The analysis presents the clinical data of a cohort. This project constitutes a major scientific effort with high methodological standards and detailed guidelines for analysis and publication to ensure scientific analyses are on the highest level. Therefore, data are not made available for the scientific community outside the established and controlled workflows and algorithms. To meet the general idea of verification and reproducibility of scientific findings, we offer access to data at the local database upon request at any time. Interested researchers should make their requests to the coordinating PI of the GPES (Achim Fieß; achim.fiess@unimedizin-mainz.de). More detailed contact information is available at the homepages of the UM (www.unimedizin-mainz.de).

Disclosure: **A. Fieß**, None; **C. Volmering**, None; **S. Gißler**, None; **E. Mildenberger**, None; **M.S. Urschitz**, None; **P. Laspas**, None; **B. Stoffelns**, None; **N. Pfeiffer**, Novartis (F), Ivantis (F), Santen (F), Thea (F), Boehringer Ingelheim Deutschland GmbH & Co. KG (F), Alcon (F), and Sanoculis (F); **A.K. Schuster**, Allergan (F), Bayer (F), Heidelberg Engineering (F), PlusOptix (F), Novartis (F), Abbvie (C), Apellis (C), Santen (C)

References

1. Blencowe H, Cousens S, Chou D, et al. Born too soon: the global epidemiology of 15 million preterm births. *Reprod Health*. 2013;10(Suppl 1):S2.
2. Fieß A, Gißler S, Mildenberger E, et al. Anterior chamber angle in adults born extremely, very, and moderately preterm with and without retinopathy of prematurity - results of the Gutenberg Prematurity Eye Study. *Children (Basel)*. 2022;9(2):281.
3. Cook A, White S, Betterbury M, Clark D. Ocular growth and refractive error development in premature infants with or without retinopathy of prematurity. *Invest Ophthalmol Vis Sci*. 2008;49(12):5199–5207.
4. Larsson EK, Rydberg AC, Holmstrom GE. A population-based study of the refractive outcome in 10-year-old preterm and full-term children. *Arch Ophthalmol*. 2003;121(10):1430–1436.
5. O'Connor AR, Stephenson TJ, Johnson A, Tobin MJ, Ratib S, Fielder AR. Change of refractive state and eye size in children of birth weight less than 1701 g. *Br J Ophthalmol*. 2006;90(4):456–460.
6. Blencowe H, Lawn JE, Vazquez T, Fielder A, Gilbert C. Preterm-associated visual impairment and estimates of retinopathy of prematurity at regional and global levels for 2010. *Pediatr Res*. 2013;74 Suppl 1(Suppl 1):35–49.
7. Fieß A, Berger LA, Riedl JC, et al. The role of preterm birth, retinopathy of prematurity and perinatal factors on corneal aberrations in adulthood: results from the Gutenberg prematurity eye study. *Ophthalmic Physiol Opt*. 2022;42(6):1379–1389.
8. Fieß A, Schuster AK, Kölb-Keerl R, et al. Corneal aberrations in former preterm infants: results from the Wiesbaden Prematurity Study. *Invest Ophthalmol Vis Sci*. 2017;58(14):6374–6378.
9. Fieß A, Kölb-Keerl R, Knuf M, et al. Axial length and anterior segment alterations in former preterm infants and full-term neonates analyzed with Scheimpflug imaging. *Cornea*. 2017;36(7):821–827.

10. Tong AY, El-Dairi M, Maldonado RS, et al. Evaluation of optic nerve development in preterm and term infants using handheld spectral-domain optical coherence tomography. *Ophthalmology*. 2014;121(9):1818–1826.
11. Åkerblom H, Holmström G, Eriksson U, Larsson E. Retinal nerve fibre layer thickness in school-aged prematurely-born children compared to children born at term. *Br J Ophthalmol*. 2012;96(7):956–960.
12. Fieß A, Pfisterer A, Gißler S, et al. Retinal thickness and foveal hypoplasia in adults born preterm with and without retinopathy of prematurity: the Gutenberg Prematurity Eye Study. *Retina*. 2022;42(9):1716–1728.
13. Yanni SE, Wang J, Chan M, et al. Foveal avascular zone and foveal pit formation after preterm birth. *Br J Ophthalmol*. 2012;96(7):961–966.
14. Mintz-Hittner HA, Knight-Nanan DM, Satriano DR, Kretzer FL. A small foveal avascular zone may be an historic mark of prematurity. *Ophthalmology*. 1999;106(7):1409–1413.
15. Falavarjani KG, Lafe NA, Velez FG, et al. Optical coherence tomography angiography of the fovea in children born preterm. *Retina*. 2017;37(12):2289–2294.
16. Legocki AT, Moshiri Y, Zepeda EM, et al. Dome-shaped macula in premature infants visualized by handheld spectral-domain optical coherence tomography. *J AAPOS*. 2021;25(3):153.e1–153.e6.
17. Kumar V, Verma S, Azad SV, et al. Dome-shaped macula - review of literature. *Surv Ophthalmol*. 2021;66(4):560–571.
18. Gaucher D, Erginay A, Lecleire-Collet A, et al. Dome-shaped macula in eyes with myopic posterior staphyloma. *Am J Ophthalmol*. 2008;145(5):909–914.
19. Flitcroft DI. The complex interactions of retinal, optical and environmental factors in myopia aetiology. *Prog Retin Eye Res*. 2012;31(6):622–660.
20. Hamad AE, Moinuddin O, Blair MP, et al. Late-onset retinal findings and complications in untreated retinopathy of prematurity. *Ophthalmol Retina*. 2020;4(6):602–612.
21. Özdemir HB, Özdek S. Late sequelae of retinopathy of prematurity in adolescence and adulthood. *Saudi J Ophthalmol*. 2022;36(3):270–277.
22. Fieß A, Fauer A, Mildenberger E, et al. Refractive error, accommodation and lens opacification in adults born preterm and full-term: results from the Gutenberg Prematurity Eye Study (GPES). *Acta Ophthalmol*. 2022;100:e1439–e1450.
23. Fieß A, Gißler S, Fauer A, et al. Short report on retinal vessel metrics and arterial blood pressure in adult individuals born preterm with and without retinopathy of prematurity: results from the Gutenberg Prematurity Eye Study. *Acta Ophthalmol*. 2022;100:e1769–e1770.
24. Fieß A, Gißler S, Mildenberger E, et al. Optic nerve head morphology in adults born extreme, very and moderate preterm with and without retinopathy of prematurity: results from the Gutenberg Prematurity Eye Study. *Am J Ophthalmol*. 2022;239:212–222.
25. Fieß A, Hufschmidt-Merizian C, Gißler S, et al. Dry eye parameters and lid geometry in adults born extremely, very, and moderately preterm with and without ROP: results from the Gutenberg Prematurity Eye Study. *J Clin Med*. 2022;11(10):2702.
26. Fieß A, Nauen H, Mildenberger E, et al. Ocular geometry in adults born extremely, very and moderately preterm with and without retinopathy of prematurity: results from the Gutenberg Prematurity Eye Study. *Br J Ophthalmol*. 2023;104:1125–1131.
27. Fieß A, Pfisterer A, Gißler S, et al. Retinal thickness and foveal hypoplasia in adults born preterm with and without retinopathy of prematurity – The Gutenberg Prematurity Eye Study. *Retina*. 2022;42:1716–1728.
28. Voigt M, Fusch C, Olbertz D. Analyse des Neugeborenenkollektivs der Bundesrepublik Deutschland 12. Mitteilung: Vorstellung engmaschiger Perzentilwerte (-kurven) für die Körpermaße Neugeborener. *Geburtsh Frauenheilk*. 2006;66:956–970.
29. Bach M, Kommerell G. Determining visual acuity using European normal values: scientific principles and possibilities for automatic measurement. *Klin Monbl Augenheilkd*. 1998;212(4):190–195.
30. Thomas MG, Kumar A, Mohammad S, et al. Structural grading of foveal hypoplasia using spectral-domain optical coherence tomography a predictor of visual acuity? *Ophthalmology*. 2011;118(8):1653–1660.
31. Müller PL, Kihara Y, Olvera-Barrios A, et al. Quantification and predictors of OCT-based macular curvature and dome-shaped configuration: results from the UK Biobank. *Invest Ophthalmol Vis Sci*. 2022;63(9):28.
32. Greenland S, Senn SJ, Rothman KJ, et al. Statistical tests, P values, confidence intervals, and power: a guide to misinterpretations. *Eur J Epidemiol*. 2016;31(4):337–350.
33. Dubis AM, Costakos DM, Subramaniam CD, et al. Evaluation of normal human foveal development using optical coherence tomography and histologic examination. *Arch Ophthalmol*. 2012;130(10):1291–1300.
34. Ellabban AA, Tsujikawa A, Muraoka Y, et al. Dome-shaped macular configuration: longitudinal changes in the sclera and choroid by swept-source optical coherence tomography over two years. *Am J Ophthalmol*. 2014;158(5):1062–1070.
35. Soudier G, Gaudric A, Gualino V, et al. Macular choroidal thickness in myopic eyes with and without a dome-shaped macula: a case-control study. *Ophthalmologica*. 2016;236(3):148–153.
36. Mehdizadeh M, Nowroozzadeh MH. Dome-shaped macula in eyes with myopic posterior staphyloma. *Am J Ophthalmol*. 2008;146(3):478; author reply 478-479.
37. Flores-Moreno I, Puertas M, Almazán-Alonso E, et al. Pathologic myopia and severe pathologic myopia: correlation with axial length. *Graefes Arch Clin Exp Ophthalmol*. 2022;260(1):133–140.
38. Fieß A, Schulze K, Grabitz SD, et al. Foveal and peripapillary choroidal thickness in adults born extremely, very, and moderately preterm with and without ROP - results from the Gutenberg Prematurity Eye Study. *Transl Vis Sci Technol*. 2022;11(7):4.
39. Park UC, Lee EK, Kim BH, Oh BL. Decreased choroidal and scleral thicknesses in highly myopic eyes with posterior staphyloma. *Sci Rep*. 2021;11(1):7987.
40. Minami S, Ito Y, Ueno S, et al. Analysis of macular curvature in normal eyes using swept-source optical coherence tomography. *Jpn J Ophthalmol*. 2020;64(2):180–186.
41. Caillaux V, Gaucher D, Gualino V, Massin P, Tadayoni R, Gaudric A. Morphologic characterization of dome-shaped macula in myopic eyes with serous macular detachment. *Am J Ophthalmol*. 2013;156(5):958–967.e1.
42. Huang LC, Zhou H, Legocki AT, et al. Choroidal thickness by handheld swept-source optical coherence tomography in term newborns. *Transl Vis Sci Technol*. 2021;10(2):27.
43. Xiang L, Zhou Y, Zhang X, et al. The characteristics of dome-shaped macula in Chinese children aged 4-6 years using optical coherence tomography angiography. *BMC Ophthalmol*. 2023;23(1):35.
44. Straub J, Steidle M, Leahy C, Bello S, Callan T, Covita A. Estimating retinal shape based on widefield optical coherence tomography and axial length measurements. *Invest Ophthalmol Vis Sci*. 2018;59(9):277.
45. Miyake M, Yamashiro K, Akagi-Kurashige Y, et al. Analysis of fundus shape in highly myopic eyes by using curvature maps constructed from optical coherence tomography. *PLoS One*. 2014;9(9):e107923.

Investigative Ophthalmology & Visual Science